Feasibility Study of a Spacecraft Surveillance System

C. A. Greenhall
Communications Systems Research Section

The International Comet Exploration spacecraft will spend 2.4 years in a solar electric propulsion stage (SEPS) cruise mode, during which the health of the spacecraft will be monitored at least once a day. Although a daily two-hour DSN pass is now planned, the same surveillance function can be carried out by a much smaller, cheaper system. The system studied here uses a commercial fast Fourier transform spectrum analyzer for noncoherent, synchronous detection of an alternating-tone signal received by a small parabolic antenna (0.8 to 3 m in diameter). Integration times vary from 3.7 to 9.5 min.

I. Proposed Surveillance Method

The proposed International Comet Exploration (ICE) spacecraft will be capable of monitoring its own health during the solar electric propulsion stage (SEPS) cruise mode. It would transmit one of several signals (five, perhaps) whose meanings range from "I'm OK" to "Help!" The signal would be detected by a small, dedicated ground receiving system. If the spacecraft says that it has a problem or if no signal is detected, then a regular DSN tracking session would be scheduled.

To reduce size, weight, and pointing accuracy requirements we shall try to make the ground antenna as small as possible. The data rate can be as low as one word (two or three bits) per hour or per day. Under these circumstances we choose noncoherent detection of a multiple frequency shift keyed (MFSK) signal by a spectrum analyzer. The main problem is acquisition of the signal, which is corrupted by oscillator phase jitter, displaced by Doppler error, and smeared by Doppler rate error. Consequently there is an upper bound on integration time, which in turn puts a lower bound on signal power, no matter how much time is nominally available for detection.

Section II and Fig. 1 describe the overall surveillance system and set down the assumptions used in the analysis. Section III and Table 1 give four numerical examples. The rest of the article (up to Section VIII) consists of back-up material. Sections IV and V derive certain mission-dependent parameters (signal power and Doppler rate error) needed by the analysis, which is carried out in Sections VI and VII. Conclusions are offered in Section VIII.

II. Design Assumptions

A conceptual sketch of a surveillance system is given in Fig. 1. We list and discuss our assumptions:

(1) The *RF signal* consists of alternating *sine-wave tones* with frequencies f_0 and f_1, each held for the *word time* T_d (but see item (8) below). Such a signal is proposed in Refs. 1 and 2 for MFSK acquisition. The difference $f_1 - f_0$, having one of several possible values, constitutes the message word. These values should be much less than *a priori* Doppler uncertainty, discussed below.

(2) *Perfect word synchronization* is assumed. The word time T_d is long enough (several minutes), the range is known well enough, and spacecraft time is accurate enough for the ground system to know when the transitions between f_0 and f_1 occur. Word sync can be refreshed whenever the regular DSN tracks the spacecraft.

(3) The *short-term frequency stability* of the spacecraft oscillator that generates the signal is specified by a plot similar to Fig. 2, which plots the square root of Allan variance, $\Delta f/f_0$, vs. integration time τ. The behavior shown is typical of quartz crystal oscillators. At τ_1 there is a transition between the behaviors $\Delta f/f_0 = \text{const}/\tau$ and $\Delta f/f_0 = \sigma_y = \text{const}$. To avoid signal power degradations above 1 dB we require

$$f_0 \sigma_y \tau_1 \leqslant 0.13 \tag{1}$$

which comes from Eq. (13) below. Typically, $\tau_1 = 0.5$ sec, in which case

$$\sigma_y \leqslant 10^{-10} \qquad \text{S-band}$$

$$\sigma_y \leqslant 3 \times 10^{-11} \qquad \text{X-band}$$

(4) The *transmitter power* is 5 W for S-band, 10 W for X-band. All the radiated power goes into the surveillance signal. At present, X-band is actually not suitable for this system (which is supposed to reduce the need for DSN tracking) because X-band downlink requires an uplink for pointing the spacecraft antenna. Nevertheless, we have provided X-band designs in case a stand-alone X-band downlink is developed.

(5) The *ground antenna* is a circular paraboloidal dish. This assumption is intended only as a starting point for other designs; a circular beam shape may not be best for this application. We shall design both tracking and nontracking systems. In a *tracking* system the antenna stays pointed at the spacecraft for the length of time required by the detection process. In a *nontracking* system the antenna is pointed at the correct declination on the meridian and the spacecraft sweeps through the beam. Thus detection time is limited by the beamwidth. The antenna has to be tilted slightly from day to day or week to week.

A GaAsFET receiver is used. See Table 2 for noise temperatures.

(6) *Doppler* and *Doppler rate* uncertainty are critical to a MFSK system. The signal must hold still long enough for it to be located. Let $\dot{v}$ be the component of vehicle acceleration provided by the SEPS. We assume a Doppler rate *error* $\dot{f}$ given by

$$\dot{f} = \frac{2\dot{v}}{\lambda} \tag{2}$$

where λ is the wavelength. This is an upper bound for the error that would occur if the SEPS were to quit entirely or even start blasting in the wrong direction. Our Doppler uncertainty bandwidth W is computed by letting $\dot{f}$ accumulate for one day:

$$W = 86400\,\dot{f} \tag{3}$$

We compute a maximum SEPS acceleration of 1.8×10^{-4} m/sec^2 during the SEPS cruise II, 1986.0 to 1988.4 (Section V below). This gives

$$\dot{f} = 0.0028 \text{ Hz/sec}, \; W = 240 \text{ Hz at S-band} \tag{4}$$

$$\dot{f} = 0.010 \text{ Hz/sec}, \; W = 870 \text{ Hz at X-band} \tag{5}$$

It is assumed that the prediction errors of all other contributions to Doppler and Doppler rate are less than these numbers. To be conservative we shall make the bandwidth of the detection system at least W. Actually, the system might be able to get by with less bandwidth because a large frequency deviation is itself cause for alarm. Therefore, a DSN tracking session would be scheduled whether or not the surveillance system finds the signal.

(7) A commercial FFT *spectrum analyzer* with 256 channels and a band analysis mode is assumed. No time window shaping is used; we found that the uniform window performs better than a hanning window. In the system of Fig. 1 we use a heterodyne frequency f_h outside the nominal uncertainty band to avoid foldover of the spectrum.

(8) The *detection strategy* uses "L-look" spectral analysis and threshold detection (Ref. 3) as follows: The bandwidth b of an analyzer channel must satisfy $256\,b > W$. Each data segment of duration $1/b$ results in a spectrum; the system sums L of these spectra and declares a signal present if the summed output of some channel exceeds a certain threshold above the average channel noise power. Thus $T_d = L/b$. Once f_0 or f_1 is found, the analyzer bandwidth can be reduced for faster detection of the other frequency. In fact, the spacecraft

might simply spend less time on f_1 than on f_0. Acquisition would be made on f_0 (perfect word sync assumed), then f_1 would be detected with a narrower bandwidth. Other schemes suggest themselves; here we shall examine only the acquisition problem.

Other assumptions about the mission appear in Sections IV and V.

III. Sample Design Parameters

Table 1 gives the numerical parameters that define four possible surveillance systems. For both S-band and X-band we have designed a tracking system and a nontracking system. The tracking systems, in which the antenna follows the spacecraft for as long as the detection system needs to see the signal, represent the lowest antenna gains consistent with a detection error probability of 10^{-4}. This minimum gain is approximately proportional to the square root of the Doppler rate error $\dot{f}$ (Eq. (29) below). Antenna diameter is 2.3 m for S-band, 0.8 m for X-band. The nontracking systems, in which the spacecraft sweeps across the stationary antenna beam, use slightly larger antennas (3 m for S-band, 1.2 m for X-band) because the reduced detection time requires more signal power. While the nontracking systems are mechanically less complex than the tracking systems, they are also less flexible and reliable because they have only one brief shot per day at the spacecraft.

No margins have been built into these designs except for those created by our approximations (positive, we hope). Actual systems might have to use antennas with higher gains and narrower beams.

IV. Power-to-Noise Ratios

Using a design control table format (Table 2), we derive the ratio P/N_0 for an ideal isotropic ground antenna, where

P = carrier power

N_0 = one-sided noise spectral density

Maximum range, 5.8×10^8 km (3.9 AU), is assumed.

The results are

$$\left(\frac{P}{N_0}\right)_{\text{iso}} = 5.4 \times 10^{-4} \text{ sec}^{-1} \qquad \text{S-band}$$

$$= 6.0 \times 10^{-4} \text{ sec}^{-1} \qquad \text{X-band}$$

V. SEPS Acceleration

Standard rocket equations (Ref. 4) give

$$\dot{v} = \frac{2P}{MgI}$$

where

$\dot{v}$ = vehicle acceleration due to rocket propulsion

P = power expended on propellant

M = vehicle mass

I = specific impulse = V/g, V = exhaust speed

g = Earth gravity, 9.8 m/sec^2

Near the end of the long SEPS cruise, just before the Tempel 2 rendezvous, 3 thrusters will be used with 10 kW available to them. We estimate $P = 5630$ W, $M = 2200$ kg, $I = 2940$ sec. Therefore,

$$\dot{v} = 1.8 \times 10^{-4} \text{ m/sec}^2$$

At the time of greatest range, 1987.7, we estimate

$$\dot{v} = 6.3 \times 10^{-5} \text{ m/sec}^2$$

To be conservative we shall design for a combination of maximum acceleration and maximum range.

VI. *L*-Look Spectral Analysis

This section is about threshold detection by a spectrum analyzer of a corrupted sine wave in white Gaussian noise. For a pure sine wave, see Ref. 3. Here, we attempt to account for the degradations due to (1) position and drift of the signal relative to nearby analyzer channels, and (2) short-term oscillator phase jitter. Our analysis is approximate and incomplete, representing the best we have been able to achieve in the time available. A rigorous treatment would be a research project. Throughout, we neglect the effects of sampling.

A. Analyzer Channel Outputs

Let X be the (suitably normalized) sum of L successive outputs of a particular analyzer channel of width b. Then X is approximately a scaled version of a noncentral chi-squared random variable with $2L$ degrees of freedom (Ref. 3). Its mean and standard deviation are approximately

$$E(X) = N_0 b + P' = N_0 b(1 + r') \tag{6}$$

$$\sigma(X) = \frac{N_0 b}{\sqrt{L}} \sqrt{1 + 2r'} \tag{7}$$

where $r' = P'/(N_0 b)$ and P' is the average signal power in the channel during the L looks. If the channel contains only noise then $r' = 0$, else

$$\left.\begin{aligned} r' &= r\, G_{pd} G_j \\ r &= \frac{P}{N_0 b} \end{aligned}\right\} \tag{8}$$

where G_{pd} is the loss (<1) from position and drift of the signal during the L looks, and G_j is the loss from short-term jitter of the spacecraft oscillator. Because these two losses are actually intertwined, they deserve a unified treatment. For the present, we simply compute them separately and multiply them.

B. Position and Drift Loss G_{pd}

This loss depends on the Doppler rate error $\dot{f}$. In time L/b the signal frequency drifts by $L\dot{f}/b$; in units of the channel width b the *drift width* is

$$\delta = \frac{L\dot{f}}{b^2} \tag{9}$$

Let the frequency origin be centered in the channel. Let mb be the signal frequency at the midpoint of the L-look time interval. If $m = 0$ the midpoint of the frequency drift is at the center of the channel; if $m = 1/2$ the drift midpoint is at an edge of the channel. We call these cases the *center case* and the *edge case*. If the drift during a single look is much smaller than b, then G_{pd} is approximately the average of $\mathrm{sinc}^2\,(\pi f/b)$ over the drift interval; thus

$$G_{pd} = G_{pd}(m, \delta) = \frac{1}{\delta} \int_{m-\delta/2}^{m+\delta/2} \left(\frac{\sin \pi u}{\pi u}\right)^2 du \tag{10}$$

C. Jitter Loss G_j

Using a spectrum analyzer, first observe a perfect sine wave whose frequency is centered in one of the channels. Then replace the sine wave by a real oscillator having the same average power. Because of short-term phase jitter, the height of the spectral peak will decrease. According to Ref. 2, measurements of S-band transmitters have placed this "spectral mean loss" between 0.3 dB and 1.5 dB. According to Ref. 5, it is difficult to include this loss in performance evaluations because little is known about the exact characteristics of phase jitter. We shall nevertheless use the information in the Allan variance plot (Fig. 2) to obtain a theoretical estimate of the jitter loss G_j. The result will put an upper bound on the long-term Allan variance σ_y^2 and a lower bound on the channel bandwidth b.

If the oscillator were modulated by either a stationary phase process $\theta(t)$ or a stationary frequency process $\dot{\theta}(t)$ the situation would be in hand because the oscillator output

$$x(t) = \cos\,[2\pi f_0 t + \theta(t) + \theta_0]$$

would be stationary. (We assume θ_0 is uniformly distributed and independent of $\theta(t)$). Assuming that $\theta(t)$ is Gaussian, Middleton (Ref. 6) and others compute the spectrum of $x(t)$ given the spectrum of $\theta(t)$ or $\dot{\theta}(t)$.

Unfortunately, the typical Allan variance behavior $\Delta f/f_0 = \sigma_y = \text{const}$ for large τ indicates the presence of nonstationary "flicker of frequency" modulation. Previous theory does not apply. Since the behavior $\Delta f/f_0 = \text{const}/\tau$ for small τ indicates that a stationary phase process is also present, we adopt the following model for $\theta(t)$:

$$\theta(t) = \phi(t) + \psi(t)$$

where $\phi(t)$ and $\psi(t)$ are independent Gaussian processes, $\phi(t)$ is stationary, and $\psi(t)$ has stationary second differences. The relevant second moment properties of $\phi(t)$ and $\psi(t)$ are characterized from Fig. 2 by

$$\sigma^2(\phi) = \frac{1}{3}(2\pi f_0 \sigma_y \tau_1)^2 \tag{11}$$

$$S_{\psi\psi}(2\pi f) = \frac{f_0^2 \sigma_y^2}{(\ln 4) f^3} \tag{12}$$

where $S_{\psi\psi}$ is the one-sided spectral density of $\psi(t)$. The $1/f^3$ spectrum has a rigorous meaning in the theory of processes with stationary nth differences. Eq. (11) does not depend on the shape of the spectrum of $\phi(t)$ as long as $1/\tau_1$ is much smaller than the bandwidth of $\phi(t)$. One obtains Eqs. (11) and (12) from conventional stationary-process formalism by integrating the Allan-variance filter response times the spectral density of $\theta(t)$.

In Appendix A we derive the following approximation for the jitter loss:

$$\ln\left(\frac{1}{G_j}\right) = (2\pi f_0 \sigma_y)^2 \left(\frac{\tau_1^2}{3} + \frac{1}{(36 \ln 4) b^2}\right) \quad (13)$$

Although the analysis is not rigorous, the author believes that Eq. (13) shows the main dependencies of the loss on the Allan-variance turnover point (τ_1, σ_y) and the channel width b. The first term on the right comes from the stationary noise $\phi(t)$ and is already well understood. The second term comes from the flicker-noise jitter $\psi(t)$; as b gets smaller, the integration time gets longer, and the effect of the low-frequency phase variations predominates.

Within the confines of the analysis, Eq. (13) actually gives an upper bound for the loss. We suggest using it as long as it indicates a loss below about 2 dB.

D. Detection Criteria

We set a detection threshold $N_0 b\eta$, where $1 < \eta < r'$. A signal is detected if the outputs of a set of adjacent channels are more than $N_0 b\eta$, and all other channel outputs are less than $N_0 b\eta$.

Fix an error probability ϵ. Anticipating the discussion below, we define z_0, z_1, and z_2 by

$$Q(z_0) = \frac{\epsilon}{n}, Q(z_1) = \epsilon, Q(z_2) = \sqrt{\epsilon} \quad (14)$$

where n is the number of channels and $Q(z)$ is the probability that a standard Gaussian is more than z.

Suppose that no channel has a signal. The probability of false detection is approximately

$$P_{FD} = nP\{X > N_0 b\eta | r' = 0\}$$

Setting $P_{FD} = \epsilon$ we obtain from Appendix B that

$$\eta = 1 + \frac{x_0}{\sqrt{L}} \quad (15)$$

where

$$x_0 = z_0 \sqrt{1 - 1/(4L)} + \frac{1}{2}(z_0^2 - 1)\sqrt{1/(4L)} \quad (16)$$

Since $N_0 b$ can be estimated as the average channel power, Eq. (15) determines the threshold.

Suppose that a signal is present. The probability that we miss it or that a spurious channel output exceeds the threshold is approximately

$$\prod_k P\{X < N_0 b\eta | r' = r'_k\} + P_{FD} \quad (17)$$

where r'_k is the effective SNR in the kth channel. We require the first term of Eq. (17) to be at most ϵ. This term depends on the drift center m and the drift width $\delta = Lf/b^2$. For a given f, δ is at our disposal but m is not. Thus our detection strategy has to work for all m. Without loss of generality we can assume $0 \leq m \leq 1/2$. Lack of time forces us to consider only the center case $m = 0$ and the edge case $m = 1/2$. Also, we assume $\delta \leq 2$ so that at most two channels have significant amounts of signal.

For the *center case* we consider only one channel in Eq. (17). Setting

$$P\{X < N_0 b\eta\} = \epsilon$$

We obtain from Appendix B that

$$\eta = 1 + r' - \frac{x_1 \sqrt{1 + 2r'}}{\sqrt{L}} \quad (18)$$

where

$$x_1 = z_1 \sqrt{1 - \beta/(4L)} - \frac{1}{2}(z_1^2 - 1)\sqrt{\beta/(4L)} \quad (19)$$

$$\beta = \frac{1 + 2r'}{(1 + r')^2} \quad (20)$$

and r' is calculated using $G_{pd}(0, \delta)$. From Eqs. (15) and (18) we get the detection criterion

$$r' = \frac{x_0 + x_1 \sqrt{1 + 2r'}}{\sqrt{L}} \quad (21)$$

for the center case.

In the *edge case* the two channels on either side of the drift midpoint $m = 1/2$ see an equal amount of signal. Therefore we set

$$[P\{X < N_0 b\eta\}]^2 = \epsilon$$

which leads as before to

$$\eta = 1 + r' - \frac{x_2\sqrt{1+2r'}}{\sqrt{L}} \tag{22}$$

where

$$x_2 = z_2\sqrt{1-\beta/(4L)} - \frac{1}{2}(z_2^2 - 1)\sqrt{\beta/(4L)} \tag{23}$$

and r' is calculated using $G_{pd}(1/2, \delta)$. The detection criterion for the edge case is

$$r' = \frac{x_0 + x_2\sqrt{1+2r'}}{\sqrt{L}} \tag{24}$$

Let ϵ, f, and b be fixed. Given δ (or L) the right sides of Eqs. (21) and (24) depend slowly on r', so they can be iterated to get the required r' for the center and edge cases. Computing $G_{pd}(m, \delta)$ ($m = 0$ and $1/2$) and G_j we get the channel SNR

$$r = \frac{P}{N_0 b} = \frac{r'}{G_{pd}G_j}$$

as two functions of δ, say $r_1(\delta)$ (center case) and $r_2(\delta)$ (edge case). Since we don't know which case holds we must choose the worst one by setting

$$r(\delta) = \max\,[r_1(\delta), r_2(\delta)] \tag{25}$$

Finally, we get the optimum values of δ and L, and the minimum required r, by minimizing Eq. (25):

$$r_{\min} = r(\delta_{\text{opt}}) = \min_{\delta \leq 2} r(\delta) \tag{26}$$

$$L_{\text{opt}} = \frac{\delta_{\text{opt}}\, b^2}{f} \tag{27}$$

In the two examples below it turns out that the point $(\delta_{\text{opt}}, r_{\min})$ is the intersection of the $r = r_1(\delta)$ and $r = r_2(\delta)$ curves (Fig. 3). For $\delta < \delta_{\text{opt}}$, $r_2(\delta)$ is larger; for $\delta > \delta_{\text{opt}}$, $r_1(\delta)$ is larger. For both examples, $\delta_{\text{opt}} = 1.6$ approximately.

We can explain this from another point of view. For a given r there is a range of L that will support detection with a given error probability. If L is too small there is not enough time to build up the signal over the noise. If L is too large the drift spreads the signal over several channels. The minimum r is the one that shrinks this L-range to a single point.

Suppose now that $r > r_{\min}$. Assume that for $\delta < \delta_{\text{opt}}$ the edge case applies: $r_2(\delta) > r_1(\delta)$. The required L can be found by iterating

$$L = \left[\frac{x_0 + x_2\sqrt{1+2r'}}{r'}\right]^2 \tag{28}$$

whose right side depends slowly on L.

E. Approximations

Put $\epsilon = 10^{-4}$, $\delta_{\text{opt}} = 1.6$, $G_{pd} = G_{pd}(1/2, 0) = 0.41$, and compute G_j from Eq. (13). Then

$$(P/N_0)_{\min} = r_{\min} b = \frac{8}{G_{pd}G_j\sqrt{\delta_{\text{opt}}}}\sqrt{f} \tag{29}$$

$$T_d = \frac{L}{b} = \left[\frac{8}{G_{pd}G_j}\right]^2 \frac{b}{\left(\frac{P}{N_0}\right)^2} \tag{30}$$

for $P/N_0 \geq (P/N_0)_{\min}$.

VII. Tracking and Nontracking Systems

A. Design Equations

From Ref. 7 we extract some nominal relationships for parabolic antennas. Let d = diameter, λ = wavelength, θ = angle off-axis. Then

On-axis gain $G_a = (7\pi/4)(d^2/\lambda^2)$

Half-power beamwidth $\theta_a = 63\,\lambda/d$ deg

Off-axis gain $G(\theta) = G_a \exp(-\ln 16\,\theta^2/\theta_a^2)$

We get the weakest possible tracking system by specifying G_a such that

$$G_a r_{\text{iso}} = r_{\min}$$

where $r_{iso} = (P/N_0)_{iso}/b$. The only *a priori* restriction on the word time $T_d = L_{opt}/b = \delta_{opt}\, b^2/\dot{f}$ is the tracking time available.

If the antenna is fixed, the spacecraft simply passing through the center of the beam, then word time is limited. We arbitrarily designate the *available antenna time* by

$$T_a = 240\,\theta_a \text{ sec}$$

the time it takes a point on the celestial equator to traverse an angle $\theta_a/2$. If the r_{min} system happens to have $T_d > T_a$ then we must increase G_a until $T_d \leqslant T_a$. This can always be done because $T_d = L/b$ is roughly proportional to $1/r^2$, whereas T_a is proportional to $1/\sqrt{r}$. We also have to account for the varying gain as the spacecraft sweeps across the beam. Since the average value of $G(\theta)/G_a$ for $|\theta| \leqslant \theta_a/2$ is 0.81, we shall simply insert this extra loss into Eq. (8). This is a makeshift adjustment, of course.

The system that makes $T_d = T_a$ can be obtained from the following iteration on δ, starting with $\delta = 1$:

$$\left.\begin{aligned} L &= \frac{\delta b^2}{\dot{f}} \\ r &= \frac{17700^2 r_{iso} b^2}{L^2} \\ r' &= 0.81\, G_j G_{pd}(1/2, \delta)\, r \\ \delta &= \frac{\dot{f}}{b^2}\left[\frac{r' L^2}{x_0 + x_2\sqrt{1+2r'}}\right]^{2/3} \end{aligned}\right\} \quad (31)$$

A $T_d = T_a$ system leaves little room for error; there are at most two chances to acquire the signal. We have computed this option simply to find out what can be done with a nontracking parabolic antenna. One might design an r_{min} system using a nontracking fan-beam antenna with the wider dimension of the beam oriented east to west. The beamwidth would allow the spacecraft to stay in the beam for several word times. The antenna would probably have to be adjusted daily in declination.

B. Derivation of the Examples

1. S-band. Recall that $\dot{f} = 0.0028$ Hz/sec, $(P/N_0)_{iso} = 5.37 \times 10^{-4}$ sec^{-1}. From Eq. (4) we choose an analyzer bandwidth of 250 Hz (the next bandwidth above 240 Hz for the analyzer we have in mind). Since we assume $n = 256$ channels, we have $b = 1$ Hz. Equation (13) with $\sigma_y = 10^{-10}$, $\tau_1 = 0.5$ sec gives $G_j = 0.81$.

To derive the r_{min} (tracking) system we plot r vs. δ for the center and edge cases (Fig. 3). The intersection gives $\delta_{opt} = 1.59$, $r_{min} = 0.925$. Then $L = \delta_{opt} b^2/\dot{f} = 568$ looks, $T_d = L/b = 568$ sec. The antenna parameters are $G_a = r_{min}/r_{iso} = 1723$, $d = 2.30$ m, $\theta_a = 3.56$ deg, and $T_a = 427$ sec.

The iteration Eq. (31) gives the $T_d = T_a$ (nontracking) system. Parameters are $\delta = 0.909$, $L = 325$ looks, $G_a = 2967$, $d = 3.02$ m, $\theta_a = 2.71$ deg, and $T_a = T_d = 325$ sec.

2. X-band. Start from $\dot{f} = 10^{-2}$ Hz/sec, $(P/N_0)_{iso} = 6.03 \times 10^{-4}$ sec^{-1}. The analyzer bandwidth is 1000 Hz, so $b = 4$ Hz. Equation (13) with $\sigma_y = 3 \times 10^{-11}$, $\tau_1 = 0.5$ sec gives $G_j = 0.81$. From Fig. 2 we get the r_{min} system: $\delta_{opt} = 1.63$, $r_{min} = 0.409$, $L = 2608$ looks, $T_d = 652$ sec, $G_a = 2715$, $d = 0.791$ m, $\theta_a = 2.83$ deg, and $T_a = 340$ sec.

The parameters of the $T_d = T_a$ system are $\delta = 0.554$, $L = 886$ looks, $G_a = 6387$, $d = 1.21$ m, $\theta_a = 1.85$ deg, and $T_a = T_d = 222$ sec.

VIII. Conclusions

Provided that certain assumptions about Doppler rate error and spacecraft oscillator phase stability are met, an alternating-tone signal from a spacecraft 4 AU away can be acquired by a ground antenna a few meters in diameter, a receiver with noise temperature of order 200 K, and a commercial 256-channel spectrum analyzer. Although our design examples assume parabolic antennas, other types such as fan-beam antennas or electronically steerable arrays should be studied, especially if one wants to avoid mechanical tracking.

Our analysis has included an estimate of the effect of oscillator flicker noise on MFSK detection. A preliminary theory with a certain amount of heuristic argument has yielded the approximation Eq. (13) for the spectral mean loss. More work on this theory is needed to improve its accuracy.

References

1. Chadwick, H. D., "Frequency Acquisition in an MFSK Receiver," *Space Programs Summary 37-52*, Vol. III, pp. 47-54, Jet Propulsion Laboratory, Pasadena, Calif., 1968.

2. Chadwick, H. D., and Springett, J. C., "Design of a Low Data Rate MFSK Communication System," *IEEE Trans. Comm. Tech.*, Vol. COM-18, pp. 740-750, 1970.

3. Levitt, B. K., "Analysis of a Discrete Spectrum Analyzer for the Detection of Radio Frequency Interference," *DSN Progress Report 42-38*, pp. 83-98, Jet Propulsion Laboratory, Pasadena, Calif., 1977.

4. Hill, P. G., and Peterson, C. R., *Mechanics and Thermodynamics of Propulsion*, Addison-Wesley, 1965.

5. Lindsey, W. C., and Simon, M. K., *Telecommunication Systems Engineering*, Prentice-Hall, 1973.

6. Middleton, D., *Introduction to Statistical Communication Theory*, McGraw-Hill, 1960.

7. Edelson, R. E., ed., *Telecommunications Systems Design Techniques Handbook*, Jet Propulsion Laboratory, Pasadena, Calif., 1972.

8. Yaglom, A. M., "Correlation Theory of Processes With Random Stationary *n*th Increments," *American Math. Soc. Translations*, Series 2, Vol. 8, pp. 87-141, 1958.

9. Abramowitz, M., and Stegun, I. A., ed., *Handbook of Mathematical Functions*, National Bureau of Standards, 1964.

Table 1. Design parameters for ICE surveillance systems

	S-band, tracking	S-band, nontracking	X-band, tracking	X-band, nontracking
Doppler rate error $\dot{f}$ (Hz/sec)	0.0028	0.0028	0.010	0.010
Spectrum analyzer bandwidth (Hz)	250	250	1000	1000
Word time T_d (sec)	570	330	650	220
Antenna gain G_a (dBi)	32.4	34.7	34.3	38.1
Antenna diameter d (m)	2.3	3.0	0.79	1.2
Half-power beamwidth θ_a (deg)	3.6	2.7	2.8	1.9

Table 2. Design control table

	S-band	X-band
1. RF power to antenna, dBm		
Transmitter power, dBm	37.0	40.0
Circuit losses, dB	-0.7	-0.7 (?)
2. High-gain antenna gain, dBi	28.5	39.7
3. Space loss, dB		
loss = $\lambda^2/(4\pi R)^2$, R = 5.8 X 10^8 km	-275.0	-286.2
λ = 0.13 m or 0.356 m		
4. Power received by isotropic antenna, dBm (1 + 2 + 3)	-210.2	-207.2
5. Noise spectral density, dBm/Hz	-177.5	-175.0
$N_0 = kT$, k = 1.38 X 10^{-20} mW sec/K		
GaAs FET front end, K	120	220
Noise from ground, cosmos, atmosphere, K	10	10
6. P/N_0, isotropic antenna, dB sec^{-1} (4 - 5)	-32.7	-32.2

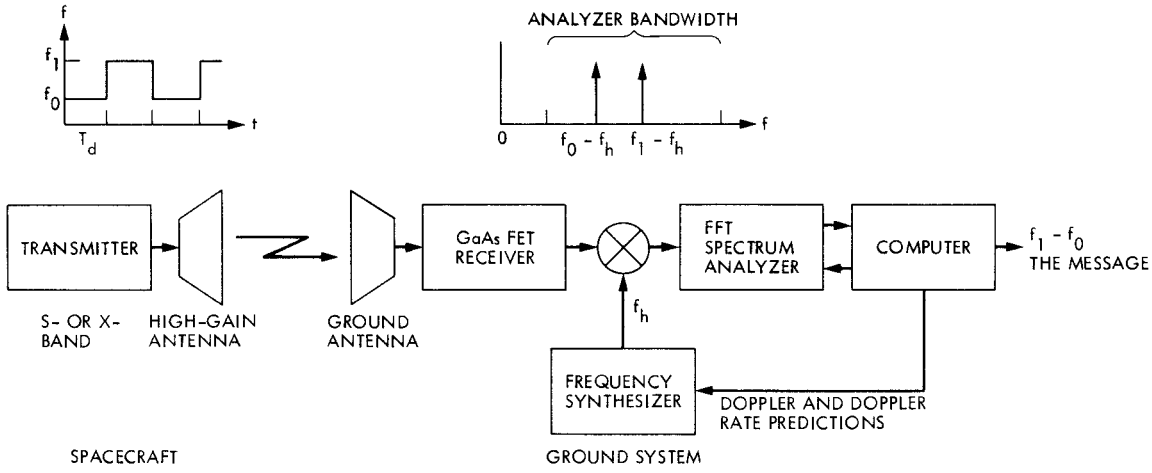

Fig. 1. Surveillance system block diagram

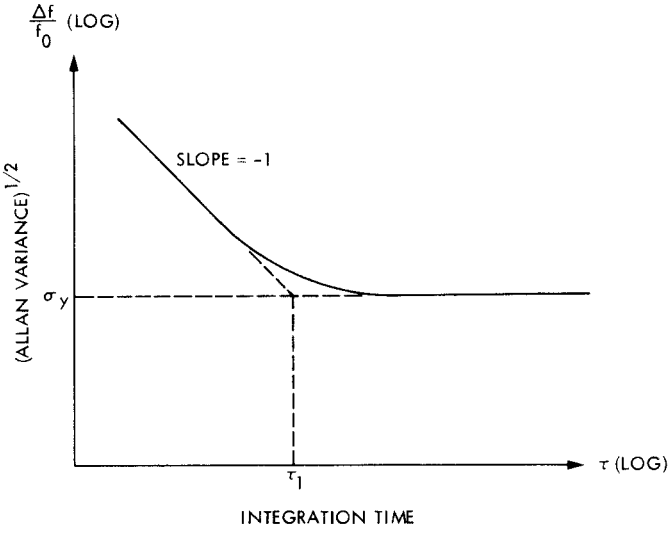

Fig. 2. Typical Allan variance plot for a quartz oscillator

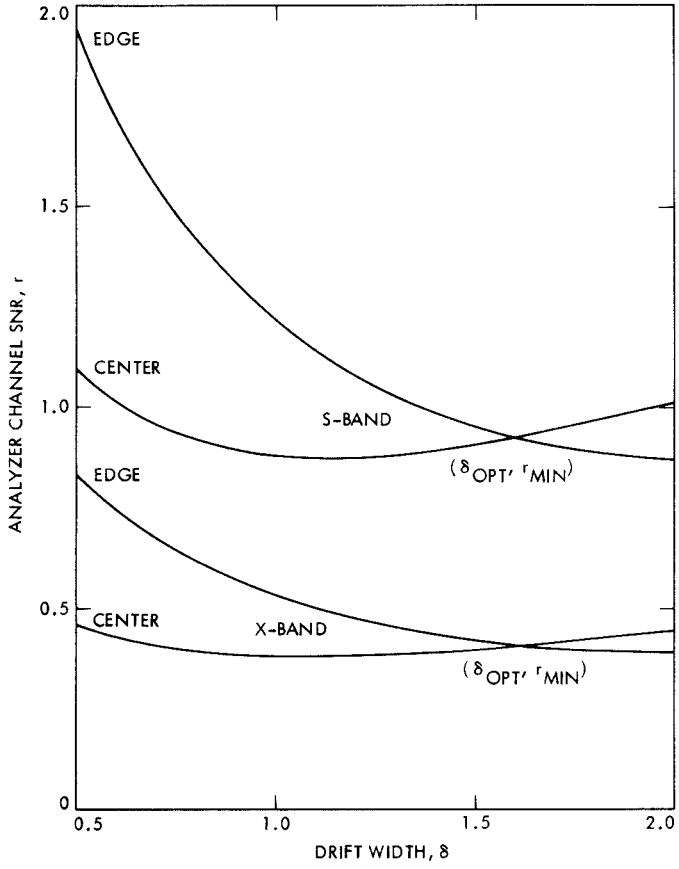

Fig. 3. Finding the minimum SNR

Appendix A

Loss From Oscillator Phase Jitter

The foundations of the second-moment theory of processes with stationary nth differences are set out by Yaglom (Ref. 8). These processes provide rigorous models for phenomena which appear to have spectral densities behaving like $1/f^{\alpha}$ as $f \to 0$, where $\alpha < 2n + 1$. For our case, $\alpha = 3$, so $n = 2$ suffices while $n = 1$ does not.

Let $\theta(t)$ (the phase of an oscillator) be a process with stationary second differences. Its spectral representation is

$$\theta(t) = a_0 + a_1 t + \frac{1}{2} ct^2 + \int_{-\infty}^{\infty} [e^{i\omega t} - 1 - F(\omega) i\omega t] \frac{dZ(\omega)}{-\omega^2} \tag{A-1}$$

where c is a constant, a_0 and a_1 are random variables, $F(\omega)$ is a bounded function satisfying

$$F(\omega) = 1 + O(|\omega|), \quad \omega \to 0$$

$$= O(1/|\omega|), \quad \omega \to \pm \infty \tag{A-2}$$

and $Z(\omega)$ is a complex-valued process with orthogonal increments, related to the two-sided spectral density $\frac{1}{2} S_{\theta\theta}(\omega)$ by

$$E|Z(\omega') - Z(\omega)|^2 = \frac{1}{2} \int_{\omega}^{\omega'} \omega^4 S_{\theta\theta}(\omega) \frac{d\omega}{2\pi} \tag{A-3}$$

The spectral density must satisfy

$$\int_{-\infty}^{\infty} \frac{\omega^4}{1 + \omega^4} S_{\theta\theta}(\omega)\, d\omega < \infty \tag{A-4}$$

We have assumed that the measure given in Eq. (A-3) (the spectrum of the generalized process $\ddot{\theta}(t)$) is absolutely continuous.

Changing $F(\omega)$ while retaining Eq. (A-2) simply adds a new component to a_1, which is just a constant of integration, a frequency offset. If one formally integrates the spectral representation of a stationary process twice, one obtains Eq. (A-1) with $F(\omega) = 1$. Such a representation for $\theta(t)$ is valid only if $\theta(t)$ has so little high-frequency power that $\dot{\theta}(t)$ exists. When one attempts to do calculations, one gets results that depend strongly on the high-frequency components of $\dot{\theta}(t)$, which we know intuitively to be irrelevant to the situation. The instantaneous oscillator frequency is perhaps meaningless. It is essential to use the correct version Eq. (A-1) with a cutoff function $F(\omega)$.

We now compute an estimate of the mean loss incurred when measuring the spectrum of an oscillator with phase $\theta(t)$. We can assume that the output has been heterodyned to baseband and that we are measuring the power in a frequency band of width b centered at zero frequency. Let $bh(bt)$ be the time window of the measurement, where h satisfies

$$h(x) = h(-x) \geq 0$$

$$\int h(x)\, dx = 1, \int x^2 h(x)\, dx < \infty$$

For later use define

$$H(y) = \int e^{ixy} h(x)\, dx$$

The mean spectral loss is given by

$$G_j = \iint E\, e^{i[\theta(s) - \theta(t)]} b^2 h(bs) h(bt)\, ds dt \tag{A-5}$$

Assume that $\theta(t)$ is a Gaussian process. Then

$$E\, e^{i[\theta(s) - \theta(t)]} = \exp\left(-\frac{1}{2} D(s,t)\right)$$

where

$$D(s,t) = E[\theta(s) - \theta(t)]^2$$

Since $b^2 h(bs) h(bt)\, ds dt$ is a positive measure with total mass 1, Jensen's Inequality gives

$$\ln \frac{1}{G_j} \leq \frac{1}{2} \iint D(s,t)\, b^2 h(bs) h(bt)\, ds dt \tag{A-6}$$

To first order in $D(s,t)$, the two sides of Eq. (A-3) are equal.

In computing $D(s,t)$ from Eq. (A-1) we assume that $c = 0$, $a_1 = 0$. The assumption $c = 0$ means that there is no average frequency drift. The assumption $a_1 = 0$ means that we don't want a constant frequency offset to affect the measurement. Also, it is convenient to replace $F(\omega)$ by $F(\omega/b)$.

Let

$$W(t,\omega) = e^{i\omega t} - 1 - i\omega t F\left(\frac{\omega}{b}\right)$$

Then

$$D(s,t) = \int_0^\infty |W(s,\omega) - W(t,\omega)|^2 S_{\theta\theta}(\omega)\frac{d\omega}{2\pi}$$

and

$$\ln\frac{1}{G_j} \leqslant \int_0^\infty V\left(\frac{\omega}{b}\right) S_{\theta\theta}(\omega)\frac{d\omega}{2\pi} \qquad \text{(A-7)}$$

where

$$V(y) = \int |e^{ixy} - H(y) - ixyF(y)|^2 h(x)\,dx$$

We still consider the function F to be at our disposal. Fixing y we find the number $F(y)$ that minimizes $V(y)$. This is done by projecting $e^{ixy} - H(y)$ onto the vector ix in the space $L^2[h(x)]$. The answer is

$$F(y) = \frac{H'(y)}{yH''(0)} \qquad \text{(A-8)}$$

$$V(y) = 1 - H(y)^2 + \frac{H'(y)^2}{H''(0)} \qquad \text{(A-9)}$$

It happens that the function F given by Eq. (A-8) satisfies Eq. (A-2). The function $V(y)$ given by Eq. (A-9) is a high-pass frequency response, and the right side of Eq. (A-7) is a "high-pass variance" of $\theta(t)$ with cutoff frequency proportional to b.

Concerning the way we have played around with F, we can say only that it seems to be the right thing to do. Since changing F only changes the offset frequency a_1 and the effect of frequency offset is covered by the loss G_{pd}, we feel free to minimize the effect of the offset on G_j. We want the average frequency during the measurement to be zero in some sense. More work on this part of the theory is needed.

Now set

$$h(y) = 1, \quad |y| \leqslant 1/2$$

$$= 0, \quad \text{elsewhere}$$

$$S_{\theta\theta}(\omega) = S_{\phi\phi}(\omega) + \frac{A}{\omega^3}$$

where $\phi(t)$ is a stationary process with bandwidth much greater than b, so that $V(\omega/b)$ passes most of the energy in $\phi(t)$. Then Eq. (A-7) becomes

$$\ln\frac{1}{G_j} \leqslant \sigma^2(\phi) + \frac{A}{2\pi b^2}\int_0^\infty V(y)\frac{dy}{y^3} \qquad \text{(A-10)}$$

By numerical integration we find that the last integral is 1/36 (approximately). Substituting for $\sigma^2(\phi)$ and A from Eqs. (11) and (12) we get Eq. (13).

Appendix B

Chi-Squared Tail Estimates

Equation 26.4.31 of Ref. 9 is used to express the tails of a noncentral (or central) χ^2 in terms of the tails of a standard Gaussian. For our situation there are $\nu = 2L$ degrees of freedom and a noncentrality parameter $\lambda = 2Lr'$ (or zero). The approximation requires $L > 50$. Let X be a scaled version of the noncentral χ^2, define $X^* = [X - E(X)]/\sigma(X)$, and let Z be a standard Gaussian. Given a probability p define x and z by

$$P\{X^* > x\} = P\{Z > z\} = p$$

Straightforward manipulation of the approximation in Ref. 9 gives the approximation

$$x = z\sqrt{1 - \beta/(4L)} + \frac{1}{2}(z^2 - 1)\sqrt{\beta/(4L)} \qquad \text{(B-1)}$$

where

$$\beta = \frac{1 + 2r'}{(1 + r')^2}$$

To get an approximation for the lefthand tail $P\{X^* < x\}$, replace x by $-x$ and z by $-z$ in Eq. (B-1). The righthand tail of X is heavier than the Gaussian tail; the lefthand tail of X is lighter.